ACS Catalysis

Research Article

pubs.acs.org/acscatalysis

# Arenesulfonic Acid-Functionalized Mesoporous Silica Decorated with Titania: A Heterogeneous Catalyst for the One-Pot Photocatalytic Synthesis of Quinolines from Nitroaromatic Compounds and Alcohols

Amer Hakki, Ralf Dillert, and Detlef W. Bahnemann

Institut für Technische Chemie, Leibniz Universität Hannover Callinstrasse 3, D-30167 Hannover, Germany

**ABSTRACT:** Acid-modified mesoporous $SiO_2$ decorated with $TiO_2$ (T-S-Ar$SO_3$H) was successfully prepared via the co-condensation of 2-(4-chlorosulfonylphenyl)ethyltrimethoxysilane (CSPTMS) and tetraethyl orthosilicate in the presence of commercially available Sachtleben Hombikat UV100 $TiO_2$ particles. The resulting bifunctional catalyst induced the efficient one-pot photocatalytic conversion of nitroaromatic compounds into polyalkylated quinolines in $O_2$-free alcoholic solutions. In this process, a simultaneous reduction of the nitro compound and an oxidation of the alcohol are induced by the photogenerated electrons and holes, respectively. An imine is then produced upon condensation of the generated aldehyde and amino compounds. The cyclization of the produced imine yielding polyalkylated quinoline was found to be catalyzed by the surface attached arene−$SO_3$H group. The newly synthesized catalyst was characterized by TEM and BET measurements, by FTIR, TGA, as well as by an acid−base titration method.

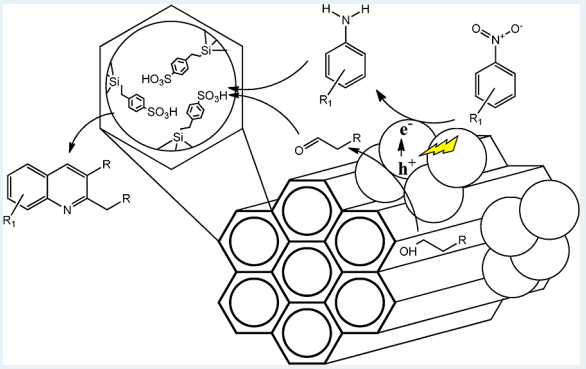

**KEYWORDS:** *photocatalysts, mesoporous materials, quinoline, reaction mechanism*

## INTRODUCTION

In terms of "green chemistry", it would be desirable if several transformations during the preparation of a complex organic compound could be performed in one sequence without the necessity of the isolation of the respective intermediates. One of the promising approaches to such types of one-pot reactions is the photocatalytic method. The well-known photoinduced charge separation occurring on the $TiO_2$ surface creates both a reduction and an oxidation center at the same time. This unique feature in principle allows multistep reactions to be carried out on a single photocatalyst.[1−8]

Quinolines and their derivatives present an important class of biologically active compounds that are prescribed as antimalarial, antibacterial, antihypertensive, and antiinflammatory drugs.[9] Furthermore, polysubstituted quinolines have been found to undergo hierarchical self-assembly into a variety of nano- and mesostructures with enhanced electronic and photonic properties.[10−12]

The most frequent routes to prepare quinolines include several named reactions, such as the Skraup,[13] Doebner−Von Miller,[14] Conrad−Limpach,[15] Friedländer,[16] and Pfitzinger[17] syntheses, all of which are based on the reaction of substituted anilines with carbonyl compounds. In conjunction with the conventional syntheses, the transition metal-catalyzed formation of quinolines has also been investigated;[18−20] however, these methods often suffer from the requirement of the prepreparation of aromatic amines and unstable carbonyl compounds; harsh reaction conditions; the use of large amounts of hazardous acids or bases; and, in particular, expensive metal complexes. Hence, the development of new strategies to obtain quinolines in a fast, clean, and efficient way has been the focus of considerable efforts. To date, only a few eco-friendly methods have been reported for the synthesis of quinoline; for example, employing ionic liquids as alternatives to volatile organic media[21] and applying supported metal nanoparticles as heterogeneous catalysts.[22−24] However, costly catalysts and relatively high reaction temperatures are still drawbacks of these methods.

We have previously reported the photocatalytic preparation of methyl quinoline using $TiO_2$ in the presence of *p*-TsOH as a cocatalyst;[6] however, the subsequent isolation of the homogeneous acid is still a problematic reaction step. The acidity of $TiO_2$ can be improved by modifying its surface using sulfate groups.[25] For example, sulfating of $TiO_2$ will result in the formation of new Brönsted acid sites on its surface, and the resulting catalysts have shown a good activity as solid acid catalysts for several acid-catalyzed reactions, such as esterification and dehydration of alcohols.[26,27] However, doubt still exists concerning the type of bonds between the sulfate groups and the surface of the $TiO_2$, that is, a leaching of $SO_4^{2-}$ groups

Received: November 15, 2012
Revised: February 2, 2013
Published: February 11, 2013

  

simply by washing with water has been reported in some cases.[27] Therefore, the development of $TiO_2$-based photocatalyst composites in which the acidic groups are strongly attached to the surface of the catalyst via strong covalent bonds is still needed.

Herein, we report for the first time a new heterogeneous "multitasking" catalyst in which the organic acid is stabilized within the pores of mesoporous silica that are also decorated with titania. Using this combination, a rapid direct synthesis of valuable quinolines from nitroaromatic compounds and alcohols under mild conditions has been successfully achieved.

$SiO_2$ has been chosen for several aspects: Firstly, for its ability to connect easily and strongly to $TiO_2$; thus, stable $TiO_2$−$SiO_2$ composites can be obtained.[28−31] Secondly, the preparation of well-ordered mesoporous silica structures with uniform pore sizes is well-known, and such materials can be easily synthesized.[32] Finally, the possibility to functionalize mesoporous silica with organic acid groups to produce promising solid acid catalysts would avoid the use of traditional homogeneous acid catalytic systems and, hence, their serious drawbacks, such as hazards in handling, corrosiveness, toxic wastes, and difficulties in separation.[33] Such solid acid catalysts have been successfully tested for a large number of acid-catalyzed reactions, such as esterification,[34−36] alkylation,[37] condensation,[38−40] and different rearrangement processes.[37,41] On the other hand, in the present work any additional problems induced by the difficulty to fabricate a $TiO_2$ photocatalyst with sufficient activity (i.e., comparable to that of commercially available $TiO_2$) have been omitted per se by employing the commercially available $TiO_2$ Sachleben Hombikat UV100, which is known to exhibit a sufficient photocatalytic performance.[42]

## EXPERIMENTAL SECTION

**Materials and Chemicals.** The commercial $TiO_2$ Hombikat UV100 powder was kindly provided by Sachtleben Chemie GmbH. 2-(4-chlorosulfonylphenyl)-ethyltrimethoxysilane (CSPTMS) 50% methylene chloride, ethanol (≥99.8%), and NaCl (≥99.99%) were obtained from Gelest, Roth, and Fluka, respectively. The block copolymer Pluronic 123, tetraethylorthosilicate (TEOS), *m*-nitrotoluene (99%), 2,7-dimethylquinoline (≥99%), HCl, and methanol were purchased from Sigma-Aldrich. All reagents were used as received. The deionized water was obtained from a Sartorius Arium 611 apparatus (18.2 MΩ cm).

**Sample Preparation.** $TiO_2$-arenesulfonic acid-functionalized mesoporous silica materials were synthesized as follows:[32] A 4 g portion of Pluronic 123 was dissolved with stirring in 125 g of 1.9 M HCl at room temperature until the complete dissolution of the surfactant, then 9.4 mL of TEOS was added dropwise. After the addition of TEOS was completed, the calculated amount of $TiO_2$ (Hombikat UV100) was added, and the resulting suspension was kept at room temperature (RT) for 45 min under stirring for prehydrolysis. Then the desired amount of CSPTMS solution in methylene chloride (50%) was added dropwise (to prevent phase separation), and the mixture was stirred at RT for 20 h, after which the mixture was aged at 100 °C for 24 h under static conditions. The template was removed from the as-synthesized material by washing with methanol and deionized water; then refluxed in ethanol for 48 h; and, finally, washed with deionized water three times, which is important to ensure that the samples are free of residual HCl used during the preparation. Bare mesoporous silica was prepared employing the same method without the addition of $TiO_2$ or CSPTMS. Samples prepared without organic acid were calcined at 450 °C under air for 4 h. The samples were labeled T(*n*)-S-Ar(*x*), where *n*:1:*x* is the molar ratio of $TiO_2$/$SiO_2$/arenesulfonic acid, respectively.

**Sample Characterization.** Fourier transform infrared spectroscopy (FTIR) spectra were recorded on a Bruker FRA 106 instrument using KBr pressed powder discs. Each sample (10 mg) was mixed with 90 mg of spectroscopically pure dry KBr and pressed into disks before its spectrum was recorded.

Thermogravimetric measurements were carried out on a Setaram Setsys evolution 1750 thermoanalyzer up to 900 °C, applying heating rates of 10 °C/min under oxygen.

Transmission electron microscopy (TEM) and high resolution transmission electron microscopy (HRTEM) measurements were carried out on a field emission transmission electron microscope of the type JEM-2100F-UHR (JEOL Ltd., Tokyo, Japan) equipped with a Gatan GIF 2001 energy filter and a 1K CCD camera. HRTEM was performed at 200 kV with an ultrahigh resolution pole piece ($C_S$ = 0.5 mm), which provides a point-resolution better than 0.19 nm. Energy dispersive X-ray (EDXS) spectra were measured with an INCA 200 EDX detector from Oxford Instruments attached to the same TEM microscope.

Single-point standard BET surface area measurements were carried out employing a Micromeritics AutoMate 23 instrument. The gas mixture of 30% nitrogen and 70% helium was used for the adsorption determinations. The $TiO_2$ samples were previously heated to 120 °C for ∼1 h to clean the surface of adsorbed humidity. The small-angle XRD diffraction patterns were acquired on a Bruker-axs D8 device using Cu K$\alpha$ radiation.

The acid capacities of the sulfonic mesoporous materials were determined using aqueous solutions of sodium chloride (NaCl, 2 M) as an ion-exchange agent. In a typical experiment, 50 mg of the solid was added to 10 mL of NaCl aqueous solution. The resulting suspension was allowed to equilibrate for 24 h and thereafter titrated potentiometrically by dropwise addition of 0.01 M KOH aqueous solution.

**Photocatalytic Reaction Procedure.** In a typical experimental run, the desired amount of the photocatalyst (equal to 25 mg of $TiO_2$) was suspended in 10 $cm^3$ of an ethanolic solution containing 100 $\mu$mol of *m*-nitrotoluene. The reaction was carried out in a double jacket Duran glass reactor with a total volume of 40 $cm^3$, which was irradiated from the outside using a 500 W mercury medium-pressure lamp, Heraeus TQ 718 Z4 (UV(A) intensity = 20 mW/$cm^2$). Before illumination, the reactor was placed in a sonicator for 3 min and then purged with Ar until no $N_2$ and $O_2$ were detected by gas chromatography (Shimadzu 8A, TCD detector) in the headspace above the solution. The reactant and the products were analyzed qualitatively and quantitatively at different illumination times after removing the semiconductor particles through filtration (0.20 $\mu$m filter) from the irradiated mixture by GC/MS and GC/FID, respectively. For GC/MS analysis, a Shimadzu gas chromatograph and mass spectrometer (Shimadzu GC/MS-QP 5000) equipped with a 30 m Rxi-5 ms (*d* = 0.32 mm) capillary column were used. Operating temperatures were programmed as follows: injection temperature, 305 °C; oven temperature, 65 °C (hold 1 min); from 65 to 120 °C at a rate of 50 °C/min, then, from 120 to 280 °C at a rate of 10 °C/min; 280 °C (hold 15 min), in split mode with split ratio of 5; injection volume (2.0 $\mu$L) with helium as a carrier gas. A


dx.doi.org/10.1021/cs300736x | ACS Catal. 2013, 3, 565−572

Shimadzu GC 2010 equipped with a Rtx-5 ($d$ = 0.25 mm) capillary column and a FID detector was used to determine the concentration of the reactant and of the products. The operating temperatures were programmed as follows: injection temperature, 250 °C; oven temperature, 70 °C (hold 2 min), from 70 to 280 °C at a rate of 10 °C/min in splitless mode. Injection volume is (2.0 $\mu$L) with nitrogen as the carrier gas.

## RESULTS AND DISCUSSION

**Characterization of the Prepared Catalysts.** The physical and chemical properties of the newlly synthesized $TiO_2$−$SiO_2$−$ArSO_3H$ catalysts, containing different $TiO_2$ and $ArSO_3H$ loadings, are summarized in Table 1.

**Table 1. The Physical and Chemical Properties of the Prepared Catalysts**

| | molar composition | | | | | |
|---|---|---|---|---|---|---|
| sample | $TiO_2$ | $SiO_2$ | Ar-$SO_3H$ | $S_{BET}$/ $m^2\ g^{-1}$ | acid capacity/ mmol $g^{-1}$ | theoretical Ar−$SO_3H$ content/ mmol $g^{-1}$ |
| $TiO_2$ | 1 | 0 | 0 | 265 | 0.02 | 0 |
| $SiO_2$ | 0 | 1 | 0 | 757 | 0.02 | 0 |
| $T_{0.1}S_1$ | 0.1 | 1 | 0 | 608 | nd[a] | 0 |
| $T_{0.5}S_1$ | 0.5 | 1 | 0 | 480 | nd. | 0 |
| $T_1S_1$ | 1 | 1 | 0 | 581 | 0.03 | 0 |
| $T_5S_1$ | 5 | 1 | 0 | 263 | nd | 0 |
| $T_{10}S_1$ | 10 | 1 | 0 | 179 | nd | 0 |
| $T_1S_1Ar_{0.03}$ | 1 | 1 | 0.03 | 424 | 0.20 | 0.20 |
| $T_1S_1Ar_{0.06}$ | 1 | 1 | 0.06 | 345 | 0.32 | 0.39 |
| $T_1S_1Ar_{0.1}$ | 1 | 1 | 0.10 | 323 | 0.50 | 0.60 |

[a]Not detected.

The transformation of chlorosulfonyl moieties into sulfonic groups mediated by acid-catalyzed hydrolysis during the preparation was confirmed by measuring the acid capacity of the sulfonic-modified materials. The acid capacity was measured by means of acid−base potentiometric titration using $Na^+$ as an ion-exchange agent. The respective results are also shown in Table 1. The close agreement between the ion-exchange capacities measured using sodium as the exchange ion with the calculated $SO_3H$ content based upon the employed concentration can be taken as clear evidence that most of the arenesulfonic groups are effectively incorporated in the silica network and are accessible and useful for catalytic conversion processes. Moreover, the decrease in the BET surface area by increasing the loaded amount of the organic acid (Table 1) clearly indicates that the acid is located on the pore wall of the mesoporous support.

Figure 1 shows the FTIR spectra of the bare oxides and of the arenesulfonic-modified $SiO_2$−$TiO_2$ samples with different Ar−$SO_3H$ molar ratios. For all the samples that contain $SiO_2$, the typical Si−O−Si stretching and bending vibration bands of the condensed silica network are present around 1210, 1080, and 794 $cm^{-1}$, whereas the peak at 956 $cm^{-1}$ corresponds to the Si−OH group.[43] The peak at 1630 $cm^{-1}$ is due to the adsorbed $H_2O$.[43] From the enlarged parts of the FTIR spectra of the bare $SiO_2$−$TiO_2$ and of the arenesulfonic-modified $SiO_2$−$TiO_2$ samples with different Ar−$SO_3H$ molar ratios (cf. I and II in Figure 1), it can be clearly seen that new bands at 1010, 1122, 1409, and 1498 $cm^{-1}$ appear only in the samples that were synthesized in the presence of CSPTMS. The intensity of these bands increases as the CSPTMS/(CSPTMS + TEOS) molar ratio in the initial mixture is increased. The two peaks at 1409 and 1498 $cm^{-1}$ are assigned to CC stretching vibrations in the aromatic ring of the embedded organic acid, whereas a weak vibration appears as a shoulder at 1600 $cm^{-1}$, corresponding also to the aromatic ring.[44] On the other hand, the two peaks at 1010 and 1122 $cm^{-1}$ are close to those of the C−H aromatic in-plan bending vibrations.[44] However, Pejov et al.[45] have reported that the bands, which are usually assigned to the C−H aromatic in-plan bending vibrations, may also be attributed to the antisymmetric $SO_3$ stretching mode and to the symmetric $SO_3$ stretching mode, respectively.

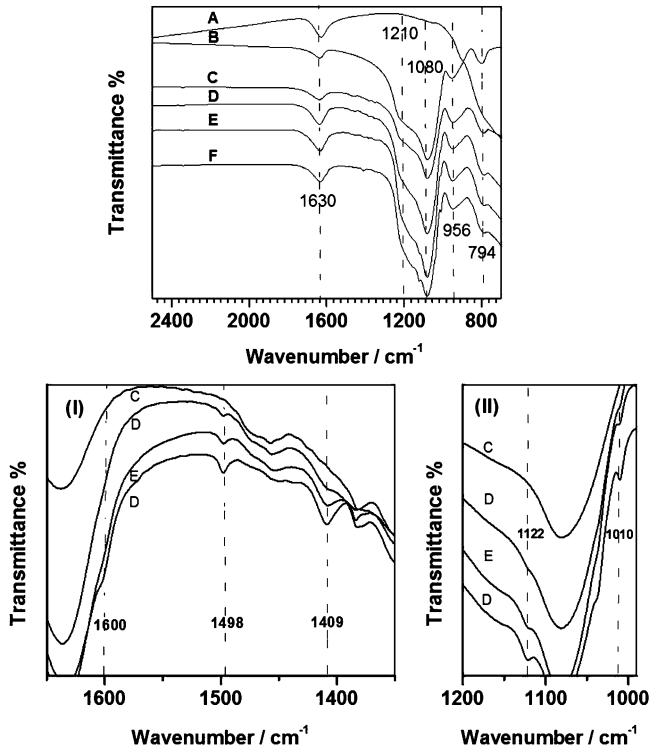


**Figure 1.** FTIR spectra of $TiO_2$ (A), $SiO_2$ (B), and extracted arenesulfonic modified $SiO_2$−$TiO_2$ samples with different Ar−$SO_3H$ molar ratios: 0 (C), 0.03 (D), 0.06 (E), 0.1 (F). Part I is the enlarged region from 1350 to 1650 $cm^{-1}$, and part II is the enlarged region from 990 to 1200 $cm^{-1}$.

TGA measurements (Figure 2) confirm the presence of the arenesulfonic acid group on the inner mesopore surfaces of the functionalized silica. A continuous mass loss with various rates is observed, which can be interpreted in combination with the DTA results. Three well-resolved regions of mass loss can be distinguished: (i) below 200 °C, (ii) between 200 and 380 °C, and (iii) above 380 °C. The first peak for each sample is associated with the desorption of physisorbed water or ethanol.[35,46,47] A peak around 280 °C is observed in both extracted samples (a, b) but not in the sample that was calcined at 450 °C for 4 h (c). This means that this peak can be attributed to the presence of residual surfactant. The decomposition of the organic acid groups was observed as two peaks in the region above 380 °C. This means that the thermal decomposition of ethylphenylsulfonic acid groups occurs in two steps starting at 418 °C and being completed at 580 °C.

EDXS imaging was used to determine the localization of each component of the prepared composite material. As can be seen from Figure 3a and b, the particles consist of a network of $SiO_2$,


dx.doi.org/10.1021/cs300736x | ACS Catal. 2013, 3, 565−572

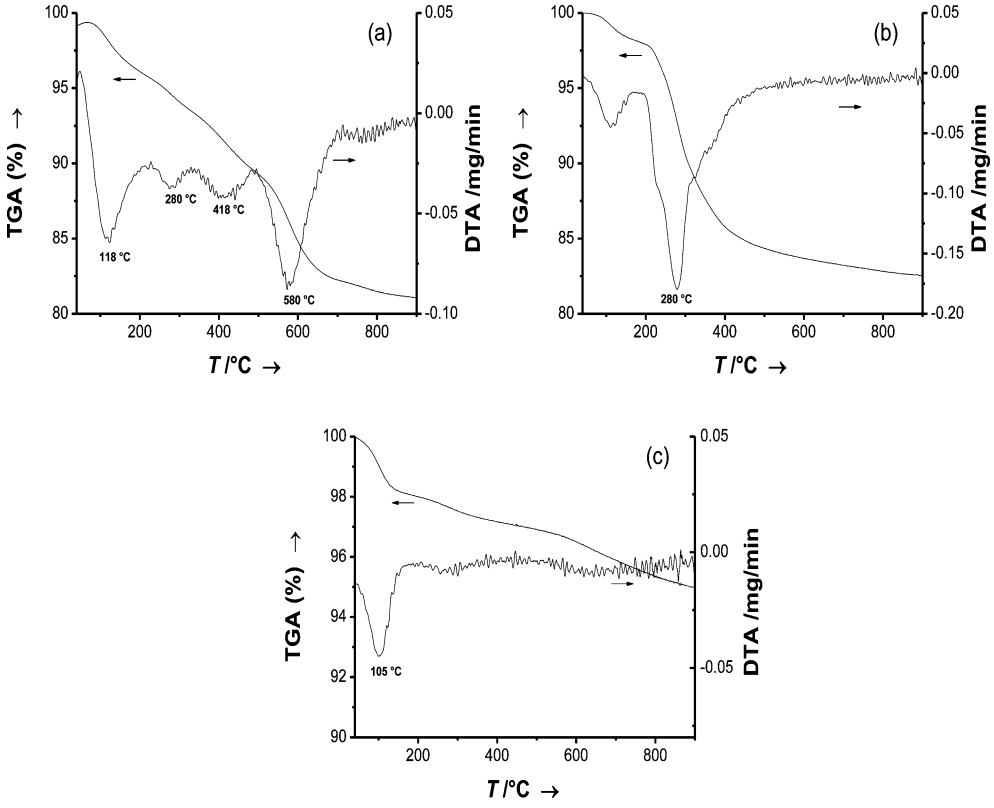


**Figure 2.** TGA and DTA measurements of (a) the extracted arenesulfonic modified $SiO_2$−$TiO_2$ sample $T_1S_1Ar_{0.1}$, (b) extracted $TiO_2$ modified with mesoporous silica, and (c) $TiO_2$ modified with mesoporous silica calcined at 450 °C for 4h.

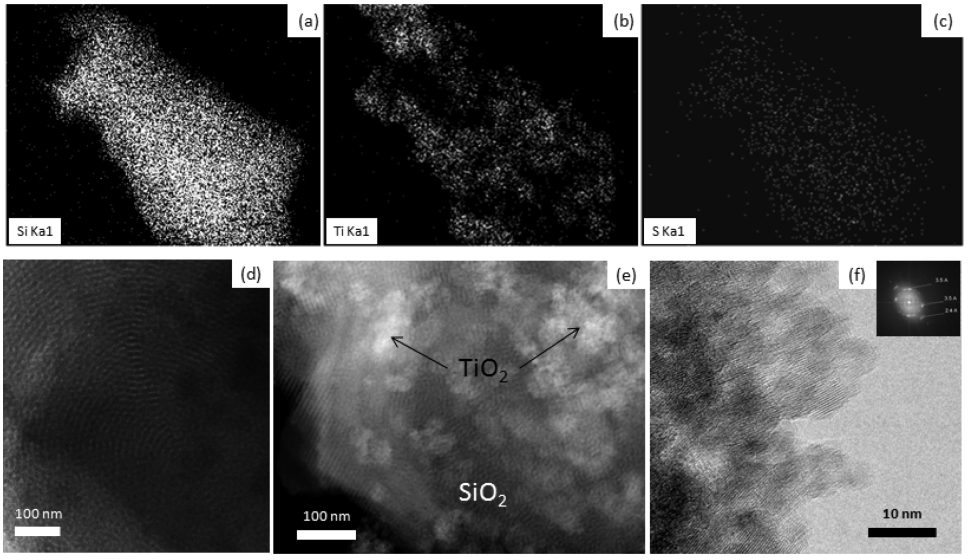


**Figure 3.** EDXS elements map of (a) silicon, (b) titanium, and (c) sulfur in the extracted arenesulfonic modified $SiO_2$−$TiO_2$ (sample $T_1S_1Ar_{0.1}$); (d) TEM image of the porous $SiO_2$ matrix in the same sample; (e) dark-field TEM micrograph showing the nanocrystalline $TiO_2$ deposited on the $SiO_2$ matrix; and (f) HRTEM image of the sample showing the anatase polycrystallites on the surface of the sample $T_1S_1Ar_{0.1}$ and the relative Fourier transformation FFT image (inset).

whereas the $TiO_2$ was located as islands of agglomerates on the surface of the $SiO_2$ particle. Furthermore, EDXS imaging (Figure 3c) shows a statistical distribution of the sulfur over the whole particle, evincing that the organic acid is not localized on just one side of the material, but delocalized over the whole $SiO_2$ matrix. The TEM images (Figure 3d, e, and f) provide clear evidence of a well ordered hexagonal structure of the porous $SiO_2$ network that is decorated with agglomerates of small (5 nm) $TiO_2$ nanoparticles (as is evident from the interlattice diffraction fringes clearly observed in the HRTEM images in Figure 3f).

To confirm the highly ordered hexagonal structure of the prepared materials, small-angle XRD analyses were carried out (Figure 4). As can be seen in Figure 4, both bare $SiO_2$ and $T_1S_1$ samples exhibit four well resolved peaks that are indexable as the (100), (110), (200), and (210) reflections associated with


dx.doi.org/10.1021/cs300736x | ACS Catal. 2013, 3, 565−572

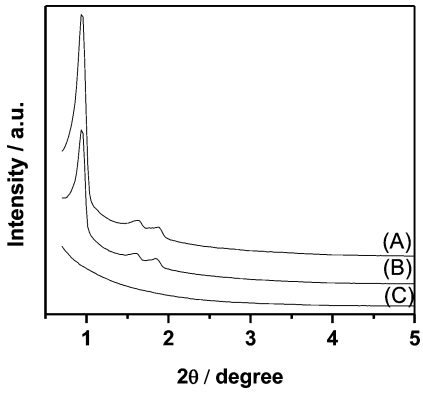


**Figure 4.** XRD patterns of (A) pure $SiO_2$, (B) $SiO_2$–$TiO_2$ (sample $T_1S_1$), and (C) the arenesulfonic modified $SiO_2$–$TiO_2$ sample $T_1S_1Ar_{0.03}$.

the *p6mm* hexagonal symmetry. The intensities of the XRD peaks of the arenesulfonic-modified sample were too low to be measurable. Such a feature, which was also reported by other research groups,[41,48] can be explained by the presence of an arenesulfonic group inside the channels of the mesoporous $SiO_2$ structure, resulting in a substantial loss in scattering contrast between the channel and the wall and, therefore, in a poor XRD pattern.

**Photocatalytic Activity for the Conversion of Nitroaromatic Compounds.** The conversion of *m*-nitrotoluene (**1a**) dissolved in ethanol was investigated as a model reaction to identify the potential of the newly prepared catalysts. Irradiation ($\lambda$ > 320 nm) of the reaction mixture under Ar at 25 °C in the presence of the acid-modified mesoporous $TiO_2$–$SiO_2$ particles resulted in the formation of 2,7-dimethylquinoline (**4a**).

Table 2 presents the results of the (**4a**) synthesis upon irradiation of (**1a**) in EtOH with the respective catalysts.

It can be clearly seen from the data presented in Table 2 that the presence of the arenesulfonic acid considerably increases the yield of the produced quinoline (**4a**). In all cases, the catalysts achieve almost total conversion of the starting nitro compound. However, bare $TiO_2$ shows considerably lower activity toward the subsequent cyclization reaction to produce the quinoline (**4a**) (cf. entry 1 in Table 2). Modifying the titania with bare $SiO_2$ is also not really sufficient to promote the yield of (**4a**) (cf. entries 2–4 in Table 2). Higher yields of (**4a**) were obtained by employing arenesulfonic acid-modified $SiO_2$–$TiO_2$ as catalysts (cf. entries 5–9 in Table 2). This enhancement in the yield of the quinoline (**4a**) is apparently due to the presence of the imbedded organic acid acting as strong Brönsted acid centers. The appearance of strong Brönsted acid centers on the silica upon modifying it with arenesulfonic groups has been previously confirmed by Melero et al.[41] by means of $^{31}P$ NMR of chemisorbed triethylphosphine oxide. The authors reported an increase in $\delta$ values from 57.9 ppm in the case of nonmodified silica, that is, corresponding to weak Lewis acid centers, to 75.0 ppm, demonstrating the presence of strong Brönsted acid centers.

In particular, $T_1S_1Ar_{0.03}$ exhibits the highest yield (52%), while increasing the organic acid amount does not result in an increased yield (see Table 2, entries 5, 8, and 9), although more accessible acid centers should be present when increasing the amount of Ar–$SO_3H$ during the preparation, as confirmed by the ion-exchange capacity and the BET measurements,

**Table 2. Conversion of *m*-Nitrotoluene and Yields of *m*-Toluidine and 2,7-Dimethylquinoline Obtained upon the Illumination of EtOH Solutions Containing *m*-Nitrotoluene and the Corresponding Catalyst[a,b]**

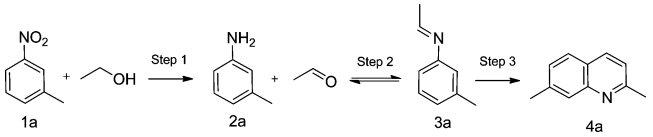


| entry | catalyst | conversion (%) | yield (%) 2a | yield (%) 4a |
|---|---|---|---|---|
| 1 | bare $TiO_2$ | 100 | 52 | 6 |
| 2 | $T_1S_1$ | 98 | 58 | 18 |
| 3 | $T_{0.5}S_1$ | 92 | 38 | 11 |
| 4 | $T_5S_1$ | 83 | 41 | 12 |
| 5 | $T_1S_1Ar_{0.03}$ | 98 | 3 | 53 |
| 6[c] | $T_1S_1Ar_{0.03(r2)}$ | 99 | 2 | 54 |
| 7[c] | $T_1S_1Ar_{0.03(r3)}$ | 99 | 3 | 53 |
| 8 | $T_1S_1Ar_{0.06}$ | 98 | 8 | 51 |
| 9 | $T_1S_1Ar_{0.1}$ | 98 | 7 | 45 |
| 10[d] | $TiO_2$ + $p$TsOH$_{10\%}$ | 97 | 3 | 45 |
| 11[d] | $TiO_2$ + $p$TsOH$_{20\%}$ | 88 | 0 | 41 |
| 12[d] | $TiO_2$ + $p$TsOH$_{40\%}$ | 93 | 9 | 39 |

[a]See Table 1. [b]Reaction conditions: catalyst (equal to 25 mg $TiO_2$), *m*-NT (100 $\mu$mol), EtOH (10 mL), 20 mW UV(A)/cm$^2$ for 4 h, 25 °C, under Ar atmosphere. [c]The suffixes r2 and r3 refer, respectively, to the second and third run of the experiment employing the same sample of the catalyst $T_1S_1Ar_{0.03}$ after washing it with deionized water and ethanol following each run. [d]Reaction conditions: 25 mg bare $TiO_2$, *m*-NT (100 $\mu$mol), EtOH (10 mL), 20 mW UV(A)/cm$^2$ for 4 h, ambient temperature, and under Ar atmosphere. *p*-Toluenesulfonic acid (*p*-TsOH) was added as $x$ = 10, 20, or 40 mol % in relation to the *m*-nitrotoluene starting amount.

respectively (see Table1). The same behavior was noticed previously when the organic acid (*p*-TsOH) was added as homogeneous cocatalyst to bare $TiO_2$ (Table 2, entries 10–12). Moreover, the prepared heterogeneous catalyst demonstrates an excellent stability and reusability, even after three catalytic runs (see Table 2, entries 5–7).

**The Proposed Reaction Mechanism.** Careful analyses for the reaction mixture at different reaction times have been performed to understand the reaction mechanism. Figure 5 shows the time course of the *m*-NT consumption as well as that of the product (**2a**, **3a**, and **4a**, respectively) formation under UVA irradiation of the reaction mixture. The time courses of the sum of the amounts of the substrate and these products are also shown in Figure 5. This summation indicates that a satisfactory material balance is kept during the reaction in the case of bare $TiO_2$, while a drop in the material balance is noticed in the case of the acid-modified catalyst ($T_1S_1Ar_{0.03}$) as a result of the formation of some byproducts or intermediates (or both), which could not be quantitatively analyzed.

The GC/MS analysis of the reaction mixtures indicates the formation of several products and intermediates, including *m*-toluidine (**2a**), *N*-ethylidene-3-methylaniline (**3a**), 4-ethoxy-2,7-dimethyl-1,2,3,4-tetrahydroquinoline (**5a**), 2,7-dimethyl-1,2-dihydroquinoline (**6a**), 2,7-dimethyl-1,2,3,4-tetrahydroquinoline (**7a**), and 2,7-dimethyl-quinoline (**4a**) (see Scheme 1).

Apparently, different transformations can be achieved during this one-pot synthesis by combining the photocatalytic action of $TiO_2$ with the catalytic action of the acid-functionalized $SiO_2$. As shown in Scheme 1, it is proposed that the reaction is


dx.doi.org/10.1021/cs300736x | ACS Catal. 2013, 3, 565–572

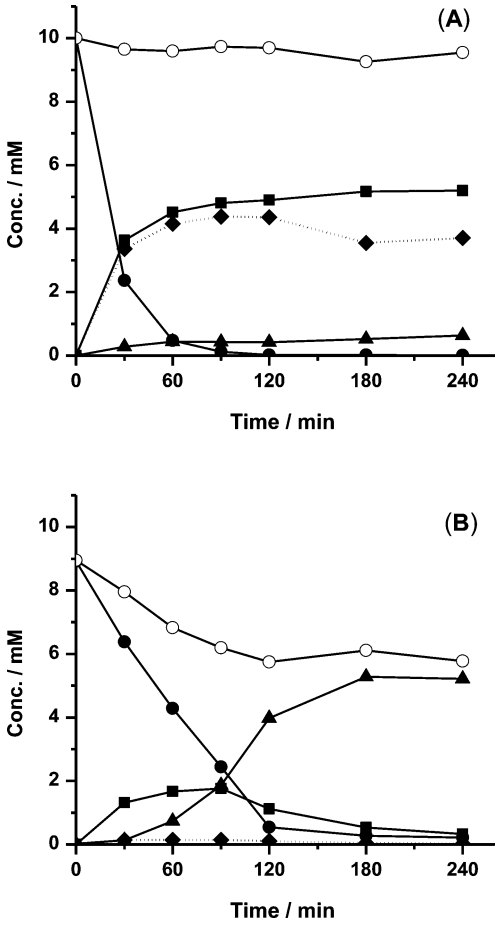


**Figure 5.** Time-dependent change in the concentrations of substrate and products during the photoirradiation of **1a** in EtOH with (A) bare $TiO_2$ or (B) $T_1S_1Ar_{0.03}$. **1a** (●), **2a** (■), **3a** (♦), **4a** (▲), and summation (○). Since the authentic imine **3a** was not available, the peak area of the imine was plotted on the calibration curve of the amine assuming that both of them have the same FID signal. The reaction conditions are given in the legend of Table 2.

initiated by the photocatalytic dehydrogenation of the alcohol to the corresponding aldehyde, consuming the photogenerated valence band holes of the illuminated $TiO_2$ and by the reduction of the nitro group of the nitroaromatic compound to an amino group induced by the photogenerated conduction band electrons. The subsequent spontaneous condensation of the aldehyde with the amino compound to produce the imine (**3a**)[49] is followed by its cyclization, which is catalyzed by the acid-functionalized $SiO_2$. The GC/MS analysis proved the intermediate formation of the imine, which, however, could not been analyzed quantitatively. Only trace amounts of *N*-ethyl-*m*-toluidine were detected by the GC or the GC/MS analysis, respectively, indicating that the newly synthesized catalysts are not able to hydrogenate the produced imine. Furthermore, following the complete consumption of the nitroaromatic compound, the color of the suspension changed to blue as a result of the trapping of photogenerated electrons by Ti(IV) to form Ti(III), indicating that no other suitable electron acceptor is present in the reaction mixture.

The presence of Brönsted acid (the imbedded $Ar-SO_3H$) in the reaction mixture may play several roles: Firstly, it will protonate the produced amino compounds as well as the surface of $TiO_2$. Therefore, both of them will be positively charged, restricting the readsorption of the product. Secondly, it will catalyze the reaction of the photocatalytically produced aldehyde with its alcohol to produce the corresponding acetal. This well-known formation of an actetal by the chemical reaction of an aldehyde with alcohol in the presence of an acid catalyst was confirmed by the detection of the acetal, **1b**, by GC/MS. If the original aldehyde carries an $\alpha$-hydrogen, an enol ether, **2b**, can be produced[50] (see Scheme 1). Cyclization of the imine with the enol ether will lead to the formation of **5a**, which can be converted to the dihydroquinoline, **6a**, upon the loss of an alcohol molecule (see Scheme 1),[51] again under the catalytic action of the stabilized Brönsted acid. Disproportionation of this dihydroquinoline (**6a**) will consequently lead to the formation of the quinoline **4a** and the tetrahydroquinoline **7a**. This mechanism can also explain why it was not possible to enhance the yield of the produced quinoline above 54%. However, this yield is still satisfying when compared with that obtained from the known conventional methods, such as Doebner–Miller[52] or Povarov.[50,53] Another advantage of employing the newly prepared catalyst is that all the transformations to produce the quinoline derivatives can be performed in one sequence without the necessity of the isolation of the intermediates.

To clarify the essential role of the light for the formation of the quinoline from the nitro aromatic compound and the alcohol, the direct conversion of the aniline (**2a**) and acetaldehyde at room temperature over $T_1S_1Ar_{0.03}$ as well as over bare $TiO_2$ was examined. For this study, the concentration of acetaldehyde was chosen to be 6 times higher than that of **2a**, assuming that in the photocatalytic reaction, the complete reduction of one nitro group to an amino group requires six electrons and six protons; hence, at least three molecules of alcohol will be oxidized to an equal number of acetaldehyde molecules. After 4 h of stirring the reaction mixture in the dark, 51% yield of the quinoline (**4a**) was obtained employing $T_1S_1Ar_{0.03}$, whereas <4% yield of this quinoline was obtained employing bare $TiO_2$ instead. This result confirms that the photocatalytic reaction steps are only the initial reduction of the nitrotoluene and the oxidation of the alcohol, whereas the condensation and the cylization reactions are catalyzed by the supported organic acid, even in the dark, i.e., these reaction steps are purely catalytic and do not require any light.

## ■ CONCLUSIONS

In summary, arenesulfonic acid-functionalized mesoporous $SiO_2$ decorated with $TiO_2$ was successfully prepared through a simple procedure using a commercially avalaible $TiO_2$ photocatalyst. The obtained catalyst was efficiently employed to convert nitroaromatic compounds into alkylated quinolines using alcohols as solvent and reactant at the same time. This conversion was achieved via the combination of the photocatalytic properties of the titanium dioxide and the acidic catalytic properties of the functionalized mesoporous silica. It was found that the formation of the corresponding aniline and aldehyde is mediated by the photocatalytic action of $TiO_2$, whereas all subsequent reactions to produce quinoline and tetrahydroquinolines via an imine, as an intermediate product, are catalyzed by the supported organic acid. An additional advantage of this functionalized photocatalyst is its ability to be recycable without any decrease in the catalytic activity. Moreover, this methodology emphasizes the green chemistry aspects of both catalysis and photocatalysis thus avoiding toxic catalysts and solvents.


dx.doi.org/10.1021/cs300736x | *ACS Catal.* 2013, 3, 565–572

**Scheme 1. Plausible Steps Involved in the Photocatalytic Conversion of Nitroaromatic Compounds to the Corresponding Quinolines**[a]

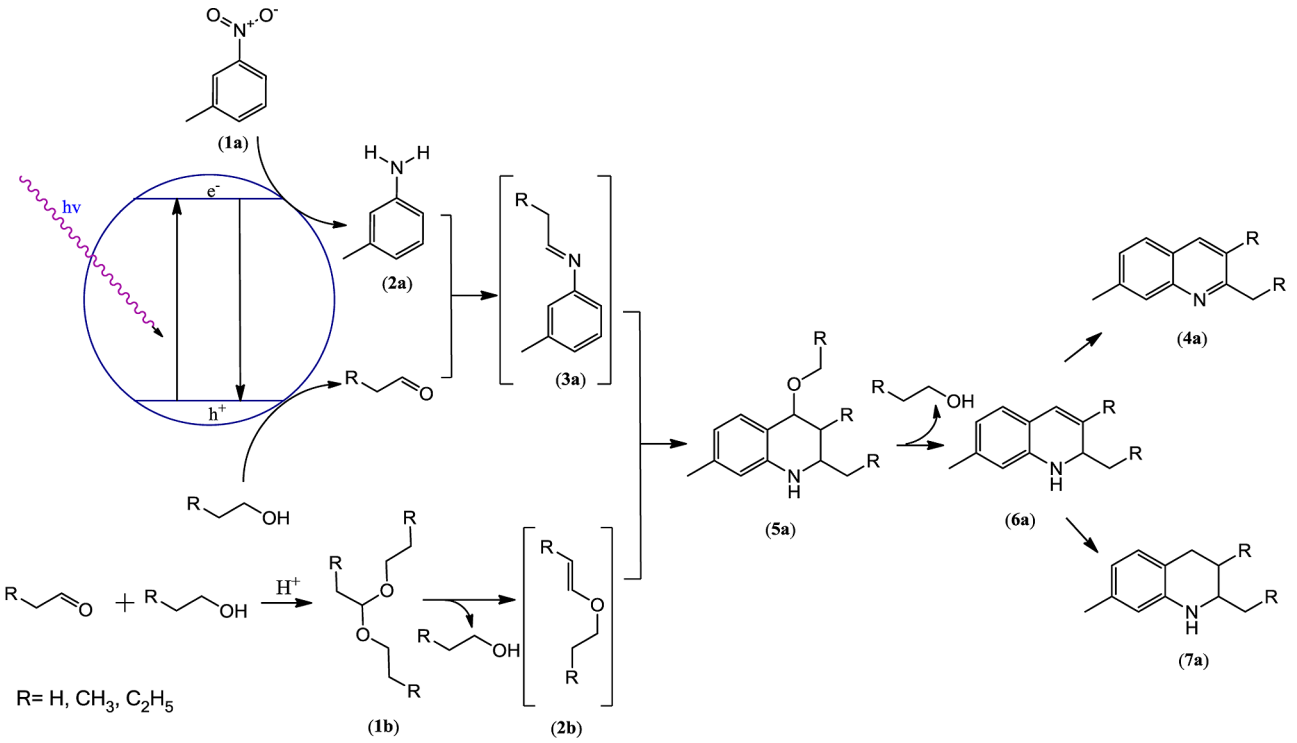


[a]All compounds except **2b** have been identified by GC or GC/MS analysis (or both).

## AUTHOR INFORMATION


### Corresponding Author

*E-mail: Bahnemann@iftc.uni-hannover.de.


### Notes

The authors declare no competing financial interest.

## ACKNOWLEDGMENTS

A.H. thanks the Deutscher Akademischer Austauschdienst (DAAD), Bonn, Germany for his Ph.D scholarship and the Department of Chemistry, Damascus University, Syria, for granting him a leave of absence. The authors thank Prof. Claus Rüscher and his team (at the Institut für Mineralogie, Leibniz Universität Hannover) for their help in the FTIR and the TGA measurements. Dr. Oliver Merka, Mr. Frank Steinbach, and Prof. Armin Feldhoff (at the Institut für Physikalische Chemie, Leibniz Universität Hannover) are also gratefully acknowledged for their support in the XRD and TEM measurements.

## REFERENCES


(1) Ohno, T.; Tsubota, T.; Kakiuchi, K.; Miyayarna, S.; Sayama, K. *J. Mol. Catal. A: Chem.* **2006**, *245*, 47−54.

(2) Lang, X. J.; Ji, H. W.; Chen, C. C.; Ma, W. H.; Zhao, J. C. *Angew. Chem., Int. Ed.* **2011**, *50*, 3934−3937.

(3) Pehlivanugullari, H. C.; Sumer, E.; Kisch, H. *Res. Chem. Intermed.* **2007**, *33*, 297−309.

(4) Park, K. H.; Joo, H. S.; Ahn, K. I.; Jun, K. *Tetrahedron Lett.* **1995**, *36*, 5943−5946.

(5) Cermenati, L.; Richter, C.; Albini, A. *Chem. Commun.* **1998**, 805−806.

(6) Hakki, A.; Dillert, R.; Bahnemann, D. *Catal. Today* **2009**, *144*, 154−159.

(7) Ohtani, B.; Osaki, H.; Nishimoto, S.; Kagiya, T. *J. Am. Chem. Soc.* **1986**, *108*, 308−310.

(8) Ohno, T.; Tokieda, K.; Higashida, S.; Matsumura, M. *Appl. Catal., A* **2003**, *244*, 383−391.

(9) Maguire, M. P.; Sheets, K. R.; McVety, K.; Spada, A. P.; Zilberstein, A. *J. Med. Chem.* **1994**, *37*, 2129−2137.

(10) Zhang, X. J.; Shetty, A. S.; Jenekhe, S. A. *Macromolecules* **1999**, *32*, 7422−7429.

(11) Ahmed, E.; Earmme, T.; Jenekhe, S. A. *Adv. Funct. Mater.* **2011**, *21*, 3889−3899.

(12) Earmme, T.; Ahmed, E.; Jenekhe, S. A. *Adv. Mater.* **2010**, *22*, 4744−4748.

(13) Manske, R. H. F.; Kulka, M. *Org. React.* **1953**, *7*, 59−98.

(14) Denmark, S. E.; Venkatraman, S. *J. Org. Chem.* **2006**, *71*, 1668−1676.

(15) Brouet, J. C.; Gu, S.; Peet, N. P.; Williams, J. D. *Synth. Commun.* **2009**, *39*, 1563−1569.

(16) Marco-Contelles, J.; Perez-Mayoral, E.; Samadi, A.; Carreiras, M. D.; Soriano, E. *Chem. Rev.* **2009**, *109*, 2652−2671.

(17) Buuhoi, N. P.; Royer, R.; Xuong, N. D.; Jacquignon, P. *J. Org. Chem.* **1953**, *18*, 1209−1224.

(18) Monrad, R. N.; Madsen, R. *Org. Biomol. Chem.* **2011**, *9*, 610−615.

(19) Cho, C. S.; Kim, T. K.; Kim, B. T.; Kim, T. J.; Shim, S. C. *J. Organomet. Chem.* **2002**, *650*, 65−68.

(20) Li, L.; Jones, W. D. *J. Am. Chem. Soc.* **2007**, *129*, 10707−10713.

(21) Akbari, J.; Heydari, A.; Kalhor, H. R.; Kohan, S. A. *J. Comb. Chem.* **2010**, *12*, 137−140.

(22) Cho, C. S.; Kim, T. G.; Yoon, N. S. *Appl. Organomet. Chem.* **2010**, *24*, 291−293.

(23) He, L.; Wang, J. Q.; Gong, Y.; Liu, Y. M.; Cao, Y.; He, H. Y.; Fan, K. N. *Angew. Chem., Int. Ed.* **2011**, *50*, 10216−10220.

(24) Selvam, K.; Swaminathan, M. *Tetrahedron Lett.* **2010**, *51*, 4911−4914.

(25) Lopez, T.; Bosch, P.; Tzompantzi, F.; Gomez, R.; Navarrete, J.; Lopez-Salinas, E.; Llanos, M. E. *Appl. Catal., A* **2000**, *197*, 107−117.

(26) Li, Z. L.; Wnetrzak, R.; Kwapinski, W.; Leahy, J. J. *ACS Appl. Mater. Interfaces* **2012**, *4*, 4499−4505.

(27) Zhao, H. Y.; Bennici, S.; Shen, J. Y.; Auroux, A. *J. Catal.* **2010**, *272*, 176−189.
(28) Ikeda, S.; Kobayashi, H.; Ikoma, Y.; Harada, T.; Torimoto, T.; Ohtani, B.; Matsumura, M. *Phys. Chem. Chem. Phys.* **2007**, *9*, 6319−6326.
(29) Oki, A. R.; Xu, Q.; Shpeizer, B.; Clearfield, A.; Qiu, X.; Kirumakki, S.; Tichy, S. *Catal. Commun.* **2007**, *8*, 950−956.
(30) Kim, Y. K.; Kim, E. Y.; Whang, C. M.; Kim, Y. H.; Lee, W. I. *J. Sol-Gel Sci. Technol.* **2005**, *33*, 87−91.
(31) Pan, J. H.; Zhao, X. S.; Lee, W. I. *Chem.—Eng. J.* **2011**, *170*, 363−380.
(32) Zhao, D. Y.; Feng, J. L.; Huo, Q. S.; Melosh, N.; Fredrickson, G. H.; Chmelka, B. F.; Stucky, G. D. *Science* **1998**, *279*, 548−552.
(33) Clark, J. H. *Acc. Chem. Res.* **2002**, *35*, 791−797.
(34) Mbaraka, I. K.; Shanks, B. H. *J. Catal.* **2006**, *244*, 78−85.
(35) Liu, J.; Yang, Q. H.; Kapoor, M. P.; Setoyama, N.; Inagaki, S.; Yang, J.; Zhang, L. *J. Phys. Chem. B* **2005**, *109*, 12250−12256.
(36) Jackson, M. A.; Mbaraka, I. K.; Shanks, B. H. *Appl. Catal., A* **2006**, *310*, 48−53.
(37) Rac, B.; Molnar, A.; Forgo, P.; Mohai, M.; Bertoti, I. *J. Mol. Catal. A: Chem.* **2006**, *244*, 46−57.
(38) Dufaud, V.; Davis, M. E. *J. Am. Chem. Soc.* **2003**, *125*, 9403−9413.
(39) Das, D.; Lee, J. F.; Cheng, S. F. *Chem. Commun.* **2001**, 2178−2179.
(40) Van Rhijn, W. M.; De Vos, D. E.; Sels, B. F.; Bossaert, W. D.; Jacobs, P. A. *Chem. Commun.* **1998**, 317−318.
(41) Melero, J. A.; Stucky, G. D.; van Grieken, R.; Morales, G. *J. Mater. Chem.* **2002**, *12*, 1664−1670.
(42) Mehrvar, M.; Anderson, W. A.; Moo-Young, M. *Int. J. Photoenergy* **2002**, *4*, 141−146.
(43) Wang, X. G.; Cheng, S. F.; Chan, J. C. C.; Chao, J. C. H. *Microporous Mesoporous Mater.* **2006**, *96*, 321−330.
(44) Xu, Z. P.; Braterman, P. S. *J. Mater. Chem.* **2003**, *13*, 268−273.
(45) Pejov, L.; Ristova, M.; Soptrajanov, B. *Spectrochim. Acta, Part A* **2011**, *79*, 27−34.
(46) Yang, Q. H.; Kapoor, M. P.; Shirokura, N.; Ohashi, M.; Inagaki, S.; Kondo, J. N.; Domen, K. *J. Mater. Chem.* **2005**, *15*, 666−673.
(47) Bibent, N.; Mehdi, A.; Silly, G.; Henn, F.; Devautour-Vinot, S. *Eur. J. Inorg. Chem.* **2011**, 3214−3225.
(48) Zhao, W.; Salame, P.; Launay, F.; Gedeon, A.; Hao, Z. *J. Porous Mater* **2008**, *15*, 139−143.
(49) Ohtani, B.; Osaki, H.; Nishimoto, S.; Kagiya, T. *Chem. Lett.* **1985**, 1075−1078.
(50) Povarov, L. S. *Russ. Chem. Rev.* **1967**, *36*, 656−670.
(51) Povarov, L. S.; Mikhailov, B. M. *Izv. Akad. Nauk SSSR, Ser. Khim.* **1964**, 2221.
(52) Leir, C. M. *J. Org. Chem.* **1977**, *42*, 911−913.
(53) Bello, D.; Ramon, R.; Lavilla, R. *Curr. Org. Chem.* **2010**, *14*, 332−356.